

3/p

N63-10174  
Model  
551013

38p



# TECHNICAL NOTE

D-1438

EFFECT OF OXIDIZER PARTICLE SIZE ON  
ADDITIVE AGGLOMERATION

By Louis A. Povinelli

Lewis Research Center  
Cleveland, Ohio

NATIONAL AERONAUTICS AND SPACE ADMINISTRATION  
WASHINGTON

November 1962

NATIONAL AERONAUTICS AND SPACE ADMINISTRATION

---

TECHNICAL NOTE D-1438

---

EFFECT OF OXIDIZER PARTICLE SIZE ON  
ADDITIVE AGGLOMERATION

By Louis A. Povinelli

SUMMARY

The effect of oxidizer particle size on additive agglomeration was investigated. Samples composed of ammonium perchlorate, polybutadiene acrylic acid, and aluminum were burned at atmospheric conditions. Agglomeration occurred when the majority of the bimodal mixture of oxidizer crystals was relatively coarse. The same propellant with predominantly fine oxidizer crystals showed no evidence of agglomeration. Particle-size distributions of the condensed-phase combustion products were obtained. The size distributions for both propellants were identical with the original additive distribution up to a particle size of approximately 8.5 microns. The agglomeration or growth of additive particles caused an apparent break in the combustion-product distribution of the coarse-oxidizer propellant; particles having diameters much larger than the original additive size were obtained. The combustion-product size distribution of the fine-oxidizer propellant did not vary from the initial additive distribution. This behavior was in agreement with the quantitative model presented for the additive growth process that predicts a step change in the agglomeration phenomenon.

The radiation characteristics of aluminized and nonaluminized propellants were obtained in emission by use of a grating spectrograph. The principal emitters were identified and interpreted relative to the agglomeration process. The strong continuum, present with the coarse-oxidizer propellant, was attributed to the presence of incandescent metallic particles on the burning surface, whereas, with the fine-oxidizer propellant, the decreased intensity of the continuum indicated that large metallic particles were not present. The burning of the additives with the latter propellant occurred throughout the flame zone, but, with the coarse propellant, the additive burning was localized to the propellant surface.

## INTRODUCTION

The aim of this investigation, conducted at the Lewis Research Center, was to gain a general knowledge of the mechanism of the combustion of metallic additives in the presence of solid-propellant burning. There is a lack of knowledge concerning the fundamental processes involved, and a need exists for investigating the various physical and chemical properties of the additive in the thin boundary (<100 microns) above the decomposing surface. Observation of phenomena occurring during combustion, for example, additive agglomeration and surface-limited combustion of the additive, adds to the knowledge necessary for understanding the role of additives.

The effect of a propellant composition variation on some basic combustion processes is described herein. Specifically, the investigation was concerned with the effect of oxidizer-particle size on additive agglomeration and with the region wherein the combustion of the additive occurs.

The knowledge gained concerning additive burning will also be useful in understanding how metallic particles suppress or assist in suppressing combustion instability. The particle size of the additive in the narrow region above the burning surface appears to be a critical parameter affecting oscillatory combustion (ref. 1).

A motion-picture film supplement has been prepared and is available on loan. A request card and a description of the film are given at the back of the report.

## THEORY

On the basis of combustion experiments using polysulfide - ammonium perchlorate propellants of unimodal particle size, it is reported in reference 2 that combustion occurs in one of several modes. The authors of reference 2 hypothesized that increasing the oxidizer particle size, within certain pressure limits, changed the mode of combustion from a premixed gaseous flame to a diffusion-type flame. This concept is employed in the present investigation, since it is assumed that the burning of the additives is controlled by the diffusion of oxygen vapors to the additive site.

In addition, it has been observed (ref. 1) that it is more difficult to suppress combustion instability by the addition of additives to coarse-oxidizer propellants than to fine-oxidizer propellants. This suggests that the oxidizer particle size may play a significant role in affecting the properties of the additives during combustion. The present investigation, therefore, is concerned with the effect of oxidizer-crystal size on additive agglomeration and burning.

### Model for Agglomeration

Consider the propellant to be composed of a matrix of uniformly spaced particles as shown in figure 1. It will be assumed that the agglomeration phenomenon is caused by the collision of additive particles on the dry, burning propellant surface. It is postulated that the particles require a finite period of time to burn, which is based on a "mixing limited" hypothesis; furthermore, the particles have a given residence or stay time on the surface and require a finite time to agglomerate. If the time to burn the larger additive is less than the agglomeration time, the molten metal burns to its oxide. Since the melting temperature of the metallic oxides generally exceeds propellant flame temperatures, agglomeration will not occur. If, however, the burning time exceeds the agglomeration time, the molten additive has an opportunity to agglomerate before it burns and forms an oxide shell.

### Burning Time

Consider the matrix of uniformly spaced oxidizer particles shown in figure 1. If  $\phi$  represents the fractional volume occupied by the oxidizer,

$$\phi = \frac{\pi}{6} n_0 d_0^3 \quad (1)$$

(Symbols are defined in the appendix.) The interparticle spacing  $\xi$  is given by the expression

$$\xi = \left( \frac{1}{n_0} \right)^{1/3} - d_0 \quad (2)$$

The combination of these expressions yields

$$\xi = d_0 \left[ \left( \frac{\pi}{6\phi} \right)^{1/3} - 1 \right] \quad (3)$$

Since the loading factor  $\phi$  is constant for any given composite mixture, the spacing between the oxidizer crystals will increase with increasing particle size within practical limits. On a microscopic level, the mixture tends to be less homogeneous with larger particles. Since the combustion mechanism presumably involves the diffusion of oxidizer vapors across the propellant surface, a local deficiency of these vapors is expected at some of the binder and additive regions of coarse-oxidizer propellants. It was assumed that the diffusion of oxidizer vapors

followed Fick's equation:

$$G_O = \mathcal{D}_{of} \frac{dc}{dx} \quad (4)$$

where  $dc/dx$  is the concentration gradient on the propellant surface between the oxidizer and additive regions. As an approximation,  $dc/dx$  is replaced by  $\Delta c/\Delta x$ , which is defined by

$$\frac{\Delta c}{\Delta x} = \frac{C_O - C_1}{\xi} \approx \frac{C_O}{\xi} \quad (5)$$

where  $C_1$  is considered negligible, since the postulated mechanism is diffusion (mixing) controlled. The rate of diffusion of oxidizer vapors is given, therefore, by

$$G_O = \mathcal{D}_{of} \frac{C_O}{\xi} \quad (6)$$

The rate may be expressed as

$$R = \frac{dM}{dt} \frac{1}{A} \quad (7)$$

where  $(dM/dt)$  is a rate of mass removal or oxygen diffusion to an additive site. The reaction rate  $R_a$  of the additive is written, therefore, from equation (7) as

$$R_a = \frac{M_a}{\tau_B} \frac{1}{S_a} \quad (8)$$

where  $\tau_B$  is the time required to burn the additive. Since the reaction is assumed to be diffusion limited, the rate of chemical reaction of the additive is determined by the rate of oxygen diffusion. Employing equations (6) and (8) results in the following:

$$\frac{M_a}{S_a} \frac{1}{\tau_B} = \mathcal{D}_{of} \frac{C_O}{\xi} \quad (9)$$

$$\tau_B = \frac{\rho}{3} \frac{\xi r_a}{\mathcal{D}_{of} C_O} \quad (10)$$

For a propellant of given oxidizer and fuel type, changes in  $\mathcal{D}_{of}$ ,  $C_o$ , and  $\rho$  with variation in oxidizer-crystal size are considered negligible; thus,

$$\tau_B \propto \xi r_a$$

The time required to burn an additive particle is proportional to the distance of closest approach of the oxidizer crystals and the additive radius.

#### Residence Time

It is assumed that the additive has a size distribution and, therefore, that the particles will have different residence times on the propellant surface. This time  $\tau_R$  is defined as the time from when an additive particle is first exposed on the surface until that particle just leaves the surface. It is assumed that the propellant surface is dry, that is, that it vaporizes without passing through the liquid phase as in the case of double-base propellants. The particle, then, leaves the surface when the binder has regressed beyond the additive, that is, when

$$t = \frac{y}{\dot{m}}$$

where  $\dot{m}$  is the regression rate of the propellant and  $y$  is the linear depth. Since  $y$  corresponds to the diameter of an additive particle  $d_a$ ,

$$\tau_R = \frac{d_a}{\dot{m}} \quad (11)$$

The residence time, therefore, increases with particle diameter, whereas higher burning rates of the propellant produce the opposite effect.

The residence time could also be influenced by the surface tension between the binder and the additive and the drag forces on the particle from the gas stream around it. If the assumption of a dry surface is invalid, the buoyancy of the additive and its ejection characteristics would have to be considered.

#### Agglomeration Time

In order to arrive at an expression for the agglomeration time, an analogy to the collision processes of molecules is employed. When it is assumed that the small (diameter) additive particles are subjected to

lateral motion and may collide with the larger particles; the collision distance  $\xi$  is

$$\xi = \left[ n_a \pi (r_1 + r_2)^2 \right]^{-1} \quad (12)$$

where  $r_2$  is the radius of the large stationary particles. If the transverse velocity  $v$  on the propellant surface is considered to be proportional to the surface regression rate and the proportionality constant is equal to the degree of turbulence,

$$v = K\dot{m} \quad (13)$$

The agglomeration time  $\tau_A$  may be written

$$\tau_A = \frac{\xi}{v} = \left[ n_a \pi K \dot{m} (r_1 + r_2)^2 \right]^{-1} \quad (14)$$

When the radius of the particles in motion is neglected,

$$\tau_A = \frac{4}{\pi K n_a d_a^2 \dot{m}} \quad (15)$$

The agglomeration time is inversely proportional to the number of particles per unit volume, the velocity of the particles, and the cross-sectional area of the particles.

The collision distance would also be influenced by the spacing of the oxidizer crystal  $\xi$ , since the additive can only be located between the crystals. Similarly, the transverse velocity could be influenced by the oxidizer spacing because of the mixing of the oxidizer and binder vapors. Since the pyrolysis rates of oxidizer and binder are different, the gas-stream velocity difference will induce shear forces with subsequent mixing. Some bubbling action of the binder might contribute to cross flow on the surface.

#### Agglomeration Criteria

In order for agglomeration to occur, the residence time of the additive particles on the surface must exceed the time required for agglomeration; that is, the ratio of equation (11) to (15) must exceed unity:

$$\frac{\tau_R}{\tau_A} > 1 \quad (16)$$

When

$$\frac{\tau_R}{\tau_A} < 1 \quad (17)$$

agglomeration will not occur. Substitution of equations (11) and (15) into equation (16) yields

$$0.785 n_a K d_a^3 > 1 \quad (18)$$

Agglomeration will occur, therefore, only when the concentration and the particle size yield values greater than unity in accordance with equation (18).

The foregoing ratio of the residence and agglomeration time, however, does not take into account the combustion of the additive, which is a simultaneous occurrence. Therefore, it is necessary to consider, in addition, the ratio of the agglomeration time to the time required to burn the additive  $\tau_B$  (eq. (10)). If the additive burning time is less than the time required for agglomeration, then the molten metal will burn and form its oxide. Since the melting point of the metallic oxides generally exceeds propellant-flame temperatures, agglomeration cannot occur. If, however, the burning time exceeds the agglomeration time, then the molten additive has an opportunity to agglomerate before it burns and forms an oxide shell on the agglomerated particle. The criterion for agglomeration consists, therefore, of the additional inequality:

$$\frac{\tau_A}{\tau_B} < 1 \quad (19)$$

If equations (10) and (15) are substituted into equation (19),

$$\frac{\pi K n_a d_a^3 \xi \dot{m} \phi}{24 \mathcal{D}_{of} C_O} > 1 \quad (20)$$

Equation (20) indicates the parametric grouping that must have a value greater than unity in order for agglomeration to occur. For a given propellant, the variation in equation (20) is confined to  $K n_a d_a^3 \xi \dot{m} \phi$ , that is, the size distribution and the concentration of the additive and oxidizer. Fixing the additive size, concentration, and type limits the variability to oxidizer spacing, propellant burning rate, and the coefficient for the cross flow  $K$ . Since increasing oxidizer size for a fixed loading  $\phi$ , increases  $\xi$  and decreases  $\dot{m}$ , the net change in



equation (20) will be small when only the oxidizer-crystal size is treated as a variable.

With fine oxidizer propellants, wherein the oxidizer spacing approaches additive size, rapid burning of the additive is expected because of the greater premixing of the ingredients. The probability of agglomeration appears remote for the fine oxidizer propellant since  $\tau_A < \tau_R$  but  $\tau_A > \tau_B$ .

#### APPARATUS AND PROCEDURE

Propellant samples made of ammonium perchlorate and polybutadiene acrylic acid were used in the investigation reported herein. The compositions used are listed in table I. The oxidizer was a blend of fine (11-micron mean weight diam.) and coarse (89-micron mean weight diam.) crystals. The particle-size distributions of the aluminum additive and oxidizers, as obtained with a micromerograph, are given in figures 2 and 3.

#### Surface Observations and Sample Collection

High-speed movies (4000 frames/sec) of the burning surface were made to determine whether agglomeration of the aluminum occurred; the propellant samples were approximately 1/2 by 3/8 by 3/16 inch. An object-to-image ratio of unity was used for the photographs, which were taken at an angle of approximately 30° to the surface. The solid combustion products were collected on Pyrex slides located 1/4-inch above the burning surface. The slides were exposed for approximately 1/20 second by use of a manually operated, sliding, slotted plate. The apparatus is shown in figure 4. No inhibitor was used on the propellant. These experiments were performed in the open air at 70°±5° F. A delay time of 1 second was used before collecting the samples in order to ensure that no pieces of the ignition wire remained in the burning region.

Size distributions of the particles collected on the slides were obtained by visual counting using high optical magnification. Only those particles that were identified as metallic or of metallic origin were counted. This procedure was necessary because of the presence of ammonium salts, binder constituents, and contaminants. An attempt to remove all the extraneous particles by oxidation at 875° K proved unsuccessful. The microscope samples were projected at a magnification of 500 on a metalloscope viewing plate and sized with the aid of an X6 eyepiece. Slightly over 1200 particles were counted for each propellant type. X-ray and electron-diffraction techniques were used to identify the major species present.

## Emission Spectra

Spectra of the various propellant compositions, both with and without the aluminum (table I), were obtained in emission with the image located on the propellant surface as shown in figure 5. This arrangement was used in the investigation reported in reference 3. The spectrograph used was a 1.5-meter Wadsworth grating instrument equipped with a 35-millimeter film holder and a remotely operated shutter. The 15,000-groove-per-inch grating gave readings of 2100 to 7800 Å in the first-order wavelength range, 2100 to 3900 Å in the second order, and 2100 to 2600 Å in the third order. Reciprocal linear dispersion at the film holder was 10.9 Å per millimeter in the first order, 5.45 Å per millimeter in the second order, and 3.63 Å per millimeter in the third order.

A quartz lens was used to focus the radiation from the burning strands on the entrance slit of the spectrograph. The spectroscopic films used, Eastman 1-0 and 1-F, were sensitive in the 2500 to 5000 Å and 2500 to 6900 Å regions, respectively. Overlap of the first and second order of the spectra occurred when the 1-F film emulsion was used.

The propellant-sample size, optical path, spectrograph slit, film exposure, and development times were maintained constant for all tests. A suitable delay time was used subsequent to ignition in order to eliminate contamination. No inhibitor was used on the propellant and, consequently, some side burning occurred. All experiments were conducted at  $70^{\circ} \pm 5^{\circ}$  F in open air.

## RESULTS AND DISCUSSION

### Agglomeration Criteria Determination

Using a value of 2.2 microns for the mean radius of the aluminum particles (fig. 2) and a 9-percent concentration (table I) and substituting for  $n_a$  in equation (18) yield

$$D > 21.4 \text{ microns} \quad (K = 0.10)$$

This critical value, approximately 20 microns, is required in order for agglomeration to occur, that is, in order to satisfy the requirement that

$$\frac{\tau_R}{\tau_A} > 1 \quad (16)$$

Since only a small number of particles of this size are present in the distribution (see fig. 2), it is expected that the agglomerates will

also be small in number. Experimental verification of this is given in the following section.

Consider now the two aluminized propellants (table I). Since the additive size distribution was constant for both propellants and the propellant type remained fixed, equation (20) reduces to

$$\beta \dot{m} \xi > 1$$

where

$$\beta = \frac{\pi K n_a d_a^3 \rho}{24 \mathcal{D}_{of} C_o}$$

The diffusion coefficient and the initial oxidizer concentration were considered invariant with change in oxidizer spacing. The diffusion coefficient was determined by use of the Chapman-Enskog relation and the Lennard-Jones function for the potential field (ref. 4) and by assuming a temperature of approximately 600° K. The resulting value is 0.35 centimeter squared per second, based on a molecular weight of 75 for the binder vapors, and 32 for the oxidizer. The density of oxygen at 1200° K was used for  $C_o$ , the oxidizer spacing was calculated from equation (3), and the burning rates were calculated or measured. For lack of better information,  $K$  was assumed constant ( $\sim 0.10$ ), although it probably increased slightly with increasing oxidizer size. Substitution in equation (20) yields

$$\beta \dot{m} \xi \approx 0.65$$

for the 70-percent fine-oxidizer propellant, and

$$\beta \dot{m} \xi \approx 1.05$$

for the 70-percent coarse-oxidizer propellant.

These values indicate that the fine-oxidizer propellant will not experience agglomeration, whereas the coarse-oxidizer propellant will undergo some additive growth. The number of particles that agglomerate will be small, as indicated by the critical agglomeration diameter. In order to test the agglomeration criteria, surface observations were made of the burning propellants and combustion products were collected.

#### Surface Observations and Sample Collection

Photographic observations. - High-speed motion pictures of the burning surface (fig. 6) revealed agglomeration of the aluminum additive

on the surface of the predominantly coarse oxidizer propellant (propellant 1 in table I). The predominantly fine oxidizer propellant (propellant 2 in table I) showed no indication of this phenomenon. Some of the aluminum particles at the center of the sample surface were observed to move laterally on the surface. The agglomeration occurred before the aluminum particles were carried off by the gas stream. It was interesting to observe that the additives served as flow tracers on the surface and that their motion indicated that somewhat unsteady conditions prevailed. This motion of the additives on the surface may have been due to their proximity to a mixing region (oxidizer-binder interface) or to sporadic bubbling and melting of the binder.

The residence times of the larger aluminum particles on the surface, discernible in the photographs, were in excess of the ignition times reported in reference 5. These larger particles, therefore, had sufficient time to ignite and burn provided that there was sufficient oxidizer present.

Similar photographs for the predominantly fine oxidizer propellant revealed only small aluminum particles on the surface that were quickly carried off by the gas stream. No agglomeration was detected. In addition, the residence time of the aluminum particles, as determined from the high-speed photographs, was appreciably lower for this fine-oxidizer mixture.

The phenomenon of surface agglomeration, which has been noticed by investigators, appears to be applicable to higher pressure combustion. In reference 6, surface agglomeration is reported to have occurred during the burning of a propellant containing ammonium perchlorate, polyurethane, and 13 percent aluminum at a chamber pressure of 400 pounds per square inch. Agglomeration or "rolling together" of molten balls of aluminum on the surface is described, but oxidizer- and additive-size distributions are not given. Data that support the findings reported herein are also reported in reference 7.

No appreciable fragmentation of the metallic combustion products, as reported in reference 8, was observed in or above the combustion zone during the present investigation.

Combustion products. - Photomicrographs of combustion products collected (fig. 7) show that the sizes of the additive after combustion were significantly larger for the predominantly coarse oxidizer propellant than for the fine-oxidizer mixture. The largest particle discernible after combustion of the fine mixture was approximately equal to the largest additive particles, whereas for the coarse-oxidizer propellant the agglomerates were significantly larger. In the latter case, the photomicrographs indicated that only a small percentage of the combustion products were agglomerates or particles of large size. The majority of

the products appeared to be of a size that was comparable with the original additive size. Some of the larger particles were hollow spheres, whereas others had solid centers. This observation was in accordance with the observations reported in reference 9. It is postulated in reference 9 that the aluminum metal was enclosed within a porous oxide coating through which oxygen diffused to burn the remaining aluminum. Similar observations are presented in reference 10.

X-ray analysis of the combustion products revealed the presence of  $\theta$ -type aluminum oxide ( $\text{Al}_2\text{O}_3$ ) as the major product species for both coarse and fine propellants. The ratios of aluminum to alumina were  $1/3$  and  $1$  for the fine- and the coarse-oxidizer propellants, respectively. These data showed that a large amount of the aluminum additive was not burned in the case of the coarse-oxidizer propellant. This result was in accordance with the proposed model, since the large interparticle spacing of the coarse-oxidizer mixture yielded a high value of burning time  $\tau_B$ , as indicated by equation (10). Increasing the value of  $\tau_B$  leads to less complete burning of the aluminum additive, since the additive may agglomerate and form an oxide shell. The large amounts of aluminum present in the combustion products were probably contained within porous oxide coatings. In the case of the fine-oxidizer propellant, where the spacing was approximately equal to mean aluminum-particle size, more complete burning occurred.

Figure 8 shows the number size distribution of the combustion particles for both fine- and coarse-oxidizer propellants. The size distribution for both propellants is represented by a single curve up to a diameter of approximately 8.5 microns. The agglomeration or growth of aluminum additive particles causes an apparent break in the distribution of the combustion products of the coarse propellant, whereas the distribution of the products of the fine-oxidizer propellant does not appear to change. Aluminum agglomeration, therefore, appears to occur only with particles larger than 8.5 microns. This result is consistent with the theoretical analysis in which the agglomeration, essentially a step function, occurs only with particles larger than a critical size of 20 microns. This correspondence between experiment and theory lends credence to the theoretical model used herein. The number distribution of the aluminum additive was determined from the weight distribution in figure 2 and is also shown in figure 8. The crossover of the fine propellant and aluminum distributions is not considered significant. The fact that the combustion product distributions below 8.5 microns are represented by a single line, which falls below the initial aluminum-additive distribution, is interpreted as meaning that most of the aluminum in the coarse-oxidizer propellant burned as completely as that in the fine-oxidizer mixture, based on percent number.

In drawing the curve, the data outside the limits of 1 and 99 percent were disregarded, and those data nearest the 50-percent level were

given preference; this is in accordance with information presented in reference 11. The data points were not weighted according to their probability levels.

Combustion-product samples collected from propellants 3 and 4, which did not contain aluminum (table I), were also analyzed; the analysis revealed the presence of ammonium chloride ( $\text{NH}_4\text{Cl}$ ) and ammonium bicarbonate ( $\text{NH}_4\text{HCO}_3$ ). This result reaffirmed the necessity of discriminating between additive and propellant products in plotting figure 8.

### Radiation Studies

Aluminized propellant. - The principal radiation from both the coarse- and the fine-oxidizer propellants (1 and 2, respectively), shown in figure 9, consists of OH bands originating at 3064 A; NH at 3360 A; CN at 3590, 3883, and 4216 A; CH at 3872 A; persistent lines of aluminum at 3082, 3093, 3944, and 3962 A; Cu at 3248 and 3274 A; Na at 3302 A; and numerous Fe lines as well as lines for Mn, K, Ga, Ni, and Cr. The spectrum of the coarse-oxidizer propellant reveals, in addition, the presence of a strong continuum beginning at approximately 3200 A. When l-F film (not shown) was used, the continuum extended far into the visible range and also revealed the sodium doublet at 5890 and 5893 A. The numerous Fe lines appear because this element is contained within the original aluminum additive. Similarly, the Cr, Cu, Ga, Mn, Ni, and some Na lines were identified with the additive by making a spectrographic analysis of the aluminum additive. In addition to the difference in the characteristics of the continuum, the fine-oxidizer propellant spectrum shows a greater number of lines throughout the entire wavelength region. At a wavelength of 3580 A, the coarse-oxidizer propellant appears to have a broad CN band, whereas the fine-oxidizer mixture exhibits the atomic lines arising from the additive elements.

These spectra (fig. 9) were obtained using the image arrangement 1 of figure 5(b) and are indicative of the streamwise distribution of emitters. The spectra show that the NH, CH, and Al emissions originate at or near the burning propellant surface; however, since relatively long exposures were required (150-micron spectrographic slit, 7 sec), it was not possible to determine whether these emitters radiate above the narrow surface region. A solution to this difficulty was to use optical arrangement 2 shown in figure 5(b). The spectra obtained (fig. 10) reveal that the CN and NH do, in fact, originate at the propellant surface. Similar observations indicated that NO,  $\text{C}_2$ , and CH originate near the propellant surface (ref. 3).

The strong continuum, present with the coarse-oxidizer propellant (fig. 10(a)), corresponds to the approximate sample dimension and is believed to be due to the presence of hot, incandescent, metallic

particles on the burning surface, as revealed in figure 6. The decreased intensity of the continuum with the fine-oxidizer mixture (fig. 10(c)) indicates that large, incandescent metallic particles were not present on the burning propellant surface, which is in accordance with the high-speed-film observations. This result is consistent with the model for the agglomeration process, since a small value of  $\xi$  and large values of  $\tau_A/\tau_B$  should lead to nonagglomerative burning.

Comparison of figures 10(a) and (c) indicates that the burning of the additive with fine-oxidizer propellant was distributed throughout the flame zone, whereas with the coarse propellant the additive burning was highly localized on the burning surface. This manner of burning is in agreement with the previously mentioned fact that a larger amount of the aluminum undergoes combustion in the case of the fine-oxidizer propellant. With the coarse-oxidizer propellant, the majority of the aluminum agglomerates and is covered with an oxide coating that prevents the additive from burning freely.

Nonaluminized propellants. - Spectra of the nonaluminized propellants (3 and 4), obtained under the same experimental conditions as the spectra of the aluminized propellants, reveal the OH bands at 3064 Å (faint), NH at 3360 Å, and CN at 3583 Å (faint) and 3883 Å. The CN and NH emissions appear to be at or near the propellant surface, and the line intensities are approximately equal.

The spectra of the nonaluminized samples do not reveal the presence of a carbon continuum; this fact supports the premise that the continuum occurring with the metallized propellant is, in fact, due to the presence of hot metal particles on the propellant surface. In reference 12, flames containing aluminum particles are reported to have continuum extending from the visible far into the ultraviolet range, AlO bands, and atomic lines of Na and Fe. The continuum was attributed to the hot incandescent particles.

The large difference in intensity between the aluminized and nonaluminized propellants is attributable to the additional energy available because of the combustion of the aluminum.

#### SUMMARY OF RESULTS

The effect of oxidizer particle size on additive agglomeration was investigated. Propellant samples composed of ammonium perchlorate, polybutadiene acrylic acid, and an aluminum additive were burned at atmospheric conditions. The percentages by weight of the oxidizer, binder, and additive were 72, 19, and 9 percent, respectively. Agglomeration of the aluminum additive on the burning propellant surface occurred when about 70 percent of the bimodal mixture of oxidizer crystals was relatively coarse and the remaining 30 percent was fine. The mean-weight

diameter of the coarse and the fine oxidizer crystals was 89 and 11 microns, respectively. Samples having the same composition but made up of 70 percent fine and 30 percent coarse oxidizer crystals showed no evidence of agglomeration.

Particle-size distributions of the condensed-phase combustion products were obtained for both the predominantly coarse and the predominantly fine oxidizer propellants. The size distributions for both propellants were identical with the original additive distribution up to a size of approximately 8.5 microns. The agglomeration caused an apparent break in the combustion-product size distribution of the coarse-oxidizer propellant; some particles had diameters as high as 100 microns. The combustion-product size distribution of the fine-oxidizer propellant did not vary from the initial additive distribution. This behavior was in quantitative agreement with the proposed theoretical model, for which it was assumed that the agglomeration phenomenon is caused by the collision of additive particles on the dry, burning propellant surface.

The time required for agglomeration was compared with the particle residence time on the surface and with the time required to burn the additive particles. If the burning time was less than the agglomeration time, which in turn was less than the residence time, then the molten metal burned to its oxide. Since the melting temperature of the metallic oxides generally exceeds propellant flame temperatures, agglomeration could not occur. If, however, the burning time exceeded the agglomeration time, then the molten additive had an opportunity to agglomerate before it burned and an oxide shell was formed.

Evaluation of the ratio of the residence time to the agglomeration time yielded the critical particle diameter of approximately 20 microns that was necessary for agglomeration to occur with the propellants used. Furthermore, the value of the agglomeration time for the coarse-oxidizer propellant was less than the burning time, whereas for the fine-oxidizer propellant, the agglomeration time exceeded the burning time. As mentioned previously, the experimental results are in agreement with the theoretical quantitative results. The critical particle diameter was found by experiment to be 8.5 microns; the theoretical value is 20 microns.

The radiation characteristics of aluminized and nonaluminized propellants were obtained in emission by use of a grating spectroscope with a first-order dispersion of 10.9 Å per millimeter. The principal emitters were identified and interpreted in terms of the agglomeration phenomenon. The strong continuum, which was present with the coarse-oxidizer propellant and which corresponded to the approximate sample dimension, was assumed to be due to the presence of hot, incandescent, metallic particles on the burning surface. The decreased intensity of the continuum with the fine-oxidizer mixture indicated that large incandescent metallic particles were not present on the burning surface. The



spectra also indicated that the additive burning occurred on the propellant surface with the coarse-oxidizer mixture, whereas the burning was distributed throughout the flame zone with the fine-oxidizer mixture. These results are in agreement with the model for agglomeration, since coarse-oxidizer propellants lead to small values of the ratio of agglomeration time to burning time. Hence, particle growth occurred on the propellant surface and impeded the aluminum from burning freely in the gas stream.

A significant decrease in intensity between the aluminized and non-aluminized propellants was observed. This variation was attributed to the additional energy that resulted from the combustion of the aluminum.

Lewis Research Center  
National Aeronautics and Space Administration  
Cleveland, Ohio, June 29, 1962

## APPENDIX - SYMBOLS

A	angstrom units
$\mathcal{A}$	diffusion area, $\text{mm}^2$
$C_0$	concentration of oxidizer vapors at oxidizer crystal, $\text{g}/\text{mm}^3$
$C_1$	concentration of oxidizer vapors at additive region, $\text{g}/\text{mm}^3$
c	concentration, $\text{g}/\text{mm}^2$
$\mathcal{D}_{\text{of}}$	diffusion coefficient of oxidizer vapors through fuel vapors, $\text{cm}^2/\text{sec}$
$d_a$	diameter of additive particle, mm
$d_0$	diameter of oxidizer crystal, mm
$G_0$	mass-flow rate per unit area of oxidizer vapors, $\text{g}/(\text{sec})(\text{mm}^2)$
K	proportionality constant
$\mathcal{L}$	collision distance, mm
M	mass, g
$M_a$	mass of additive, g
$\dot{m}$	burning or regression rate of propellant, $\text{mm}/\text{sec}$
$n_a$	number of additive particles per unit volume, $\text{mm}^{-3}$
$n_0$	number of oxidizer particles per unit volume, $\text{mm}^{-3}$
R	flux rate, $\text{g}/(\text{sec})(\text{mm}^2)$
$R_a$	reaction rate of additive, $\text{g}/(\text{sec})(\text{mm}^2)$
$r_a$	radius of additive particle, mm
$r_1$	radius of particle undergoing transverse motion, mm

$r_2$	particle radius, mm
$S_a$	surface area of additive, $\text{mm}^2$
$t$	time, sec
$v$	transverse velocity, mm/sec
$x$	direction parallel to propellant surface, mm
$y$	direction normal to propellant surface, mm
$\beta$	constant, $\frac{\pi K n_a d_a^3 \rho}{24 \mathcal{D}_{O_2} C_O}$
$\xi$	interparticle oxidizer spacing, mm
$\rho$	density of additive particle, $\text{g}/\text{mm}^3$
$\tau_A$	agglomeration time, sec
$\tau_B$	time required to burn additive, sec
$\tau_R$	residence time, time particle is exposed to surface, sec
$\phi$	fractional volume occupied by oxidizer or oxidizer loading factor

## REFERENCES

1. McClure, F. T., et al.: First Report of the Working Group on Solid Propellant Combustion Instability - A General Review of Our State of Knowledge. TG 371-1, Appl. Phys. Lab., Johns Hopkins Univ., July 1960.
2. Bastress, E. K., Hall, K. P., and Summerfield, M.: Modification of the Burning Rates of Solid Propellants by Oxidizer Particle Size Control. Paper 1597-61, Am. Rocket Soc., Inc., 1961.
3. Summerfield, Martin, et al.: Burning Mechanism of Ammonium Perchlorate Propellants. Prog. in Astronautics and Rocketry. Vol. 1. Solid Propellant Rocket Res., Academic Press, 1960, pp. 141-182.
4. Bird, R. B., Stewart, W. E., and Lightfoot, E. N.: Transport Phenomena. John Wiley & Sons, Inc., 1960.
5. Friedman, Raymond, and Macek, Andrej: Ignition and Combustion of Aluminum Particles in Hot Ambient Gases. Paper 61-21, Western States Section, Combustion Inst., Sept. 1961.
6. Watermeier, L.: An Experimental Study of Combustion Instability in Solid Rocket Propellants, pt. II. Rep. 1116, Ballistic Res. Lab., Aberdeen Proving Ground, Sept. 1960.
7. Anderson, S. E., et al.: Quarterly Progress Report on Interior ballistics. Rep. P-61-13, Rohm and Haas Co., Dec. 15, 1961.
8. Gordon, Derck A.: Combustion Characteristics of Metal Particles. Prog. in Astronautics and Rocketry. Vol. 1. Solid Propellant Rocket Res., Academic Press, 1960, pp. 271-278.
9. Fassell, W. M., Papp, C. A., Hildenbrand, D. L., and Sernka, R. P.: The Experimental Nature of the Combustion of Metallic Powders. Prog. in Astronautics and Rocketry. Vol. 1. Solid Propellant Rocket Res., Academic Press, 1960, pp. 259-269.
10. Shanfield, H., and Baum, E.: Study of Resonance Behavior in Solid Propellants - Tenth Quarterly Report. Pub. C-930, Aeronutronic, July 15, 1960.
11. Kottler, F.: The Distribution of Particle Sizes. Jour. Franklin Inst., vol. 250, no. 4, Oct. 1950, pp. 339-356.
12. Wolfhard, H. G., and Parker, W. G.: Temperature Measurements of Flames Containing Incandescent Particles. Proc. Phys. Soc. (London), ser. B, vol. 62, no. 356, Aug. 1, 1949, pp. 523-529.

TABLE I. - PROPELLANT COMPOSITIONS

Propellant	Binder, PBAA, <sup>a</sup> weight percent	Oxidizer, ammonium perchlorate, weight percent		Additive, aluminum, weight percent
		Fine	Coarse	
1	19	16.5	55.5	9
2	19	55.5	16.5	9
3	19	18.5	62.5	-
4	19	62.5	18.5	-

<sup>a</sup>Polybutadiene acrylic acid (epoxy crosslinked copolymer of butadiene and a carboxylic monomer).

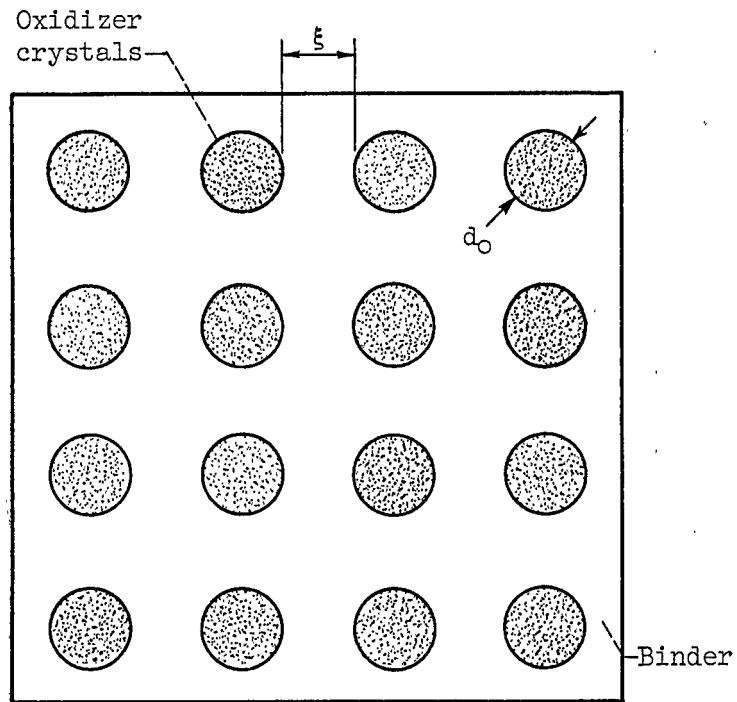


Figure 1. - Simplified matrix model for composite propellant. Interparticle spacing,  $\xi$ ; particle diameter,  $d_o$ .

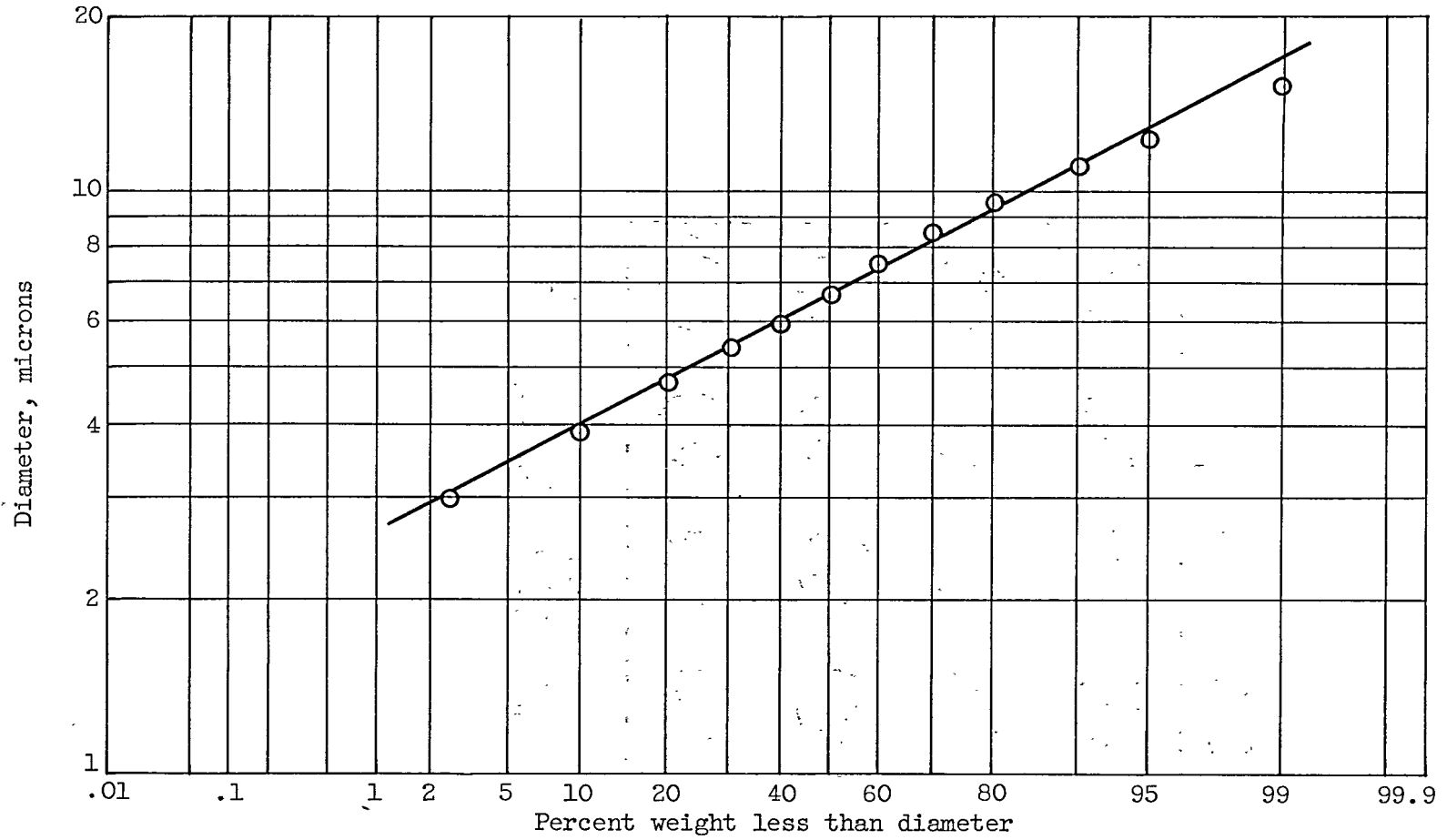


Figure 2. - Aluminum particle-size distribution.

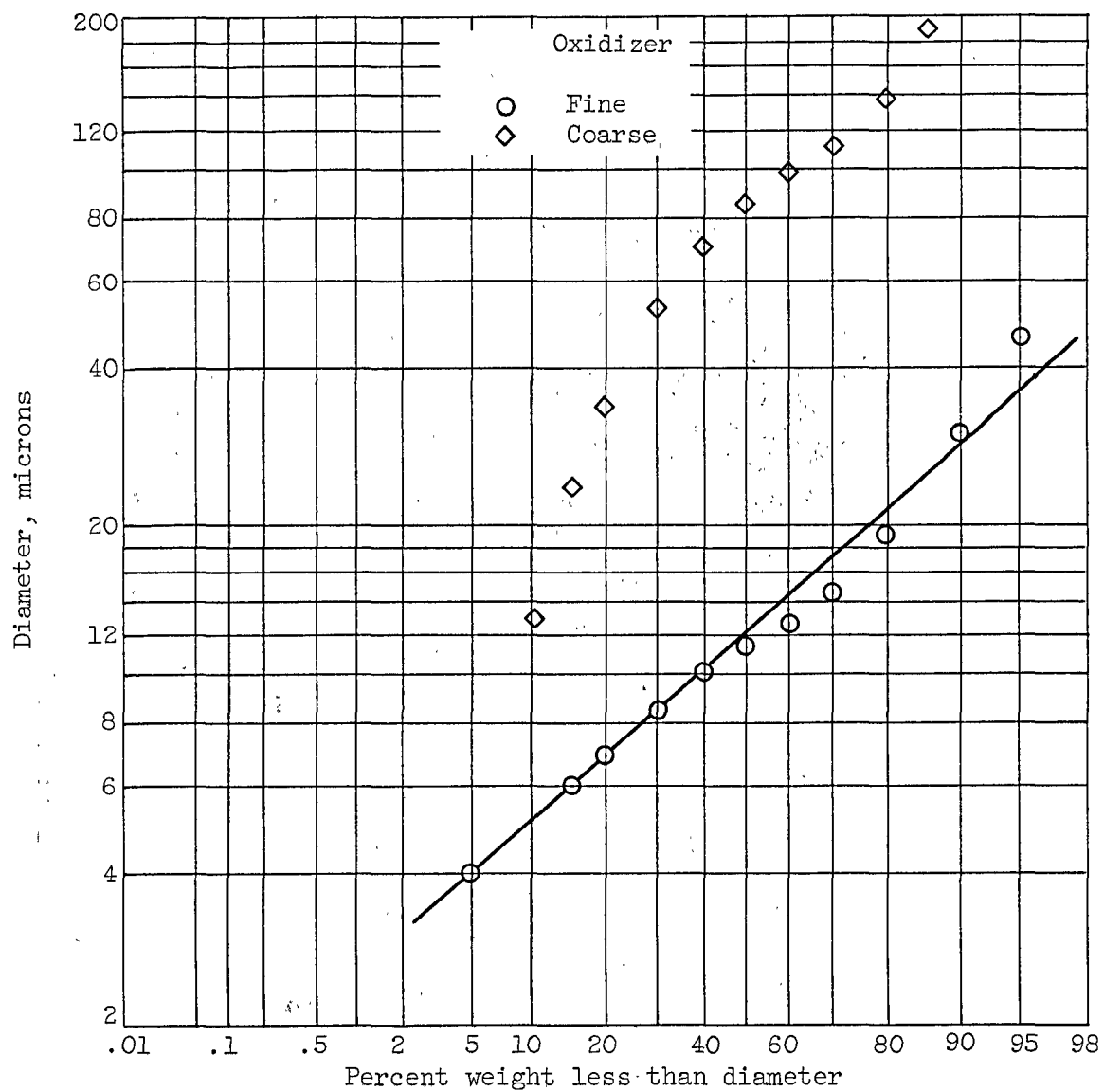


Figure 3. - Oxidizer particle-size distribution.



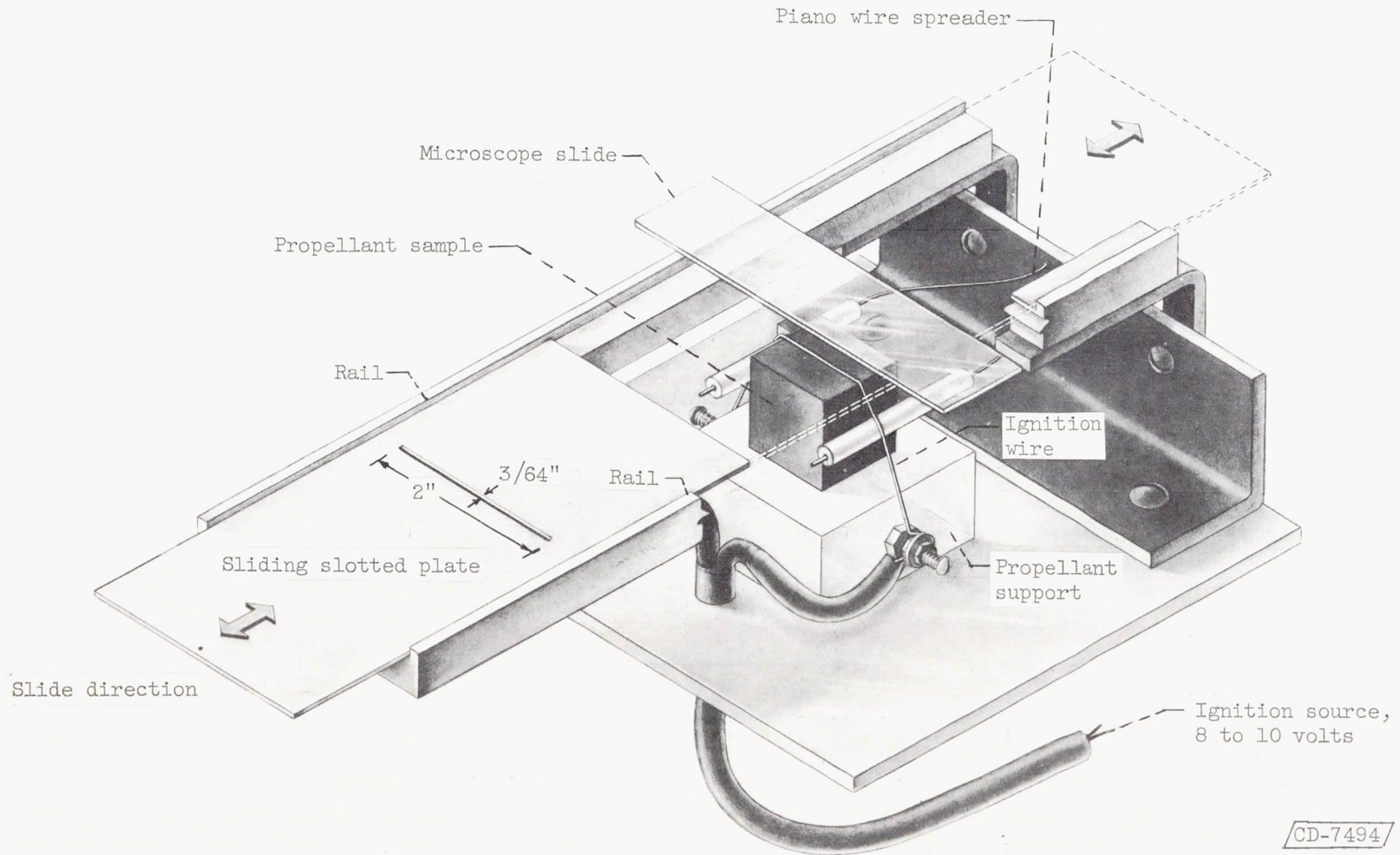
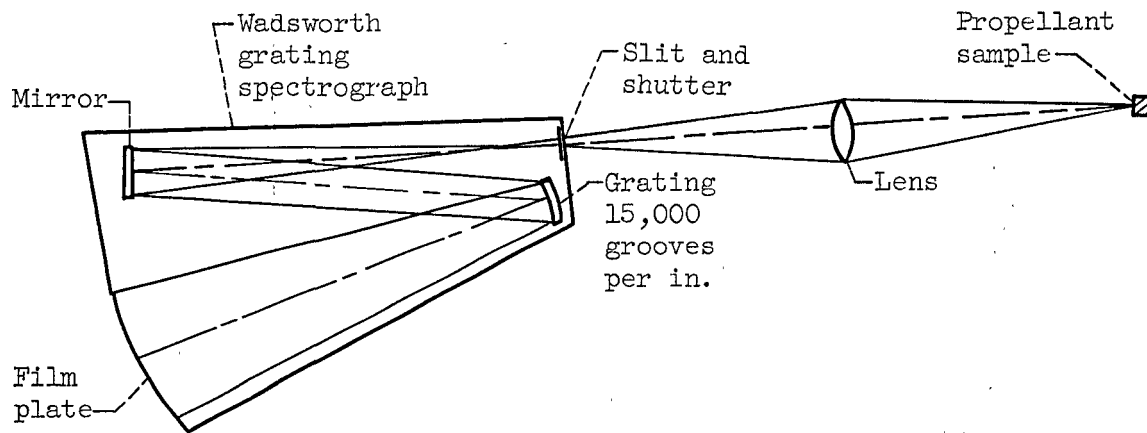
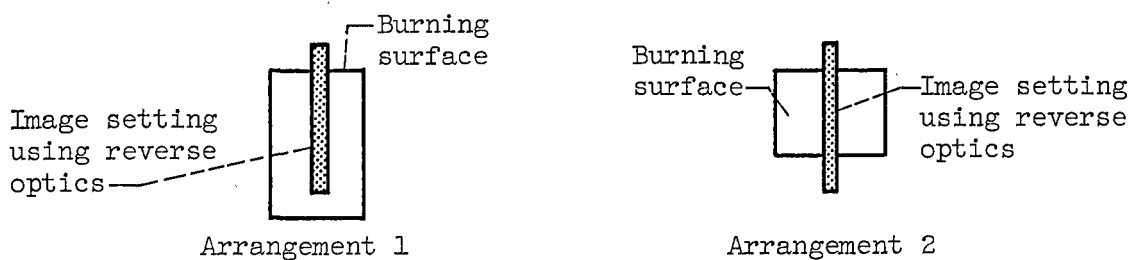


Figure 4. - Experimental apparatus for collecting combustion sample.



(a) Schematic diagram of optical system.



(b) Arrangements of propellant and slit.

Figure 5. - Optical arrangement for spectrographic observations and positioning of image for streamwise distribution and lateral distribution.

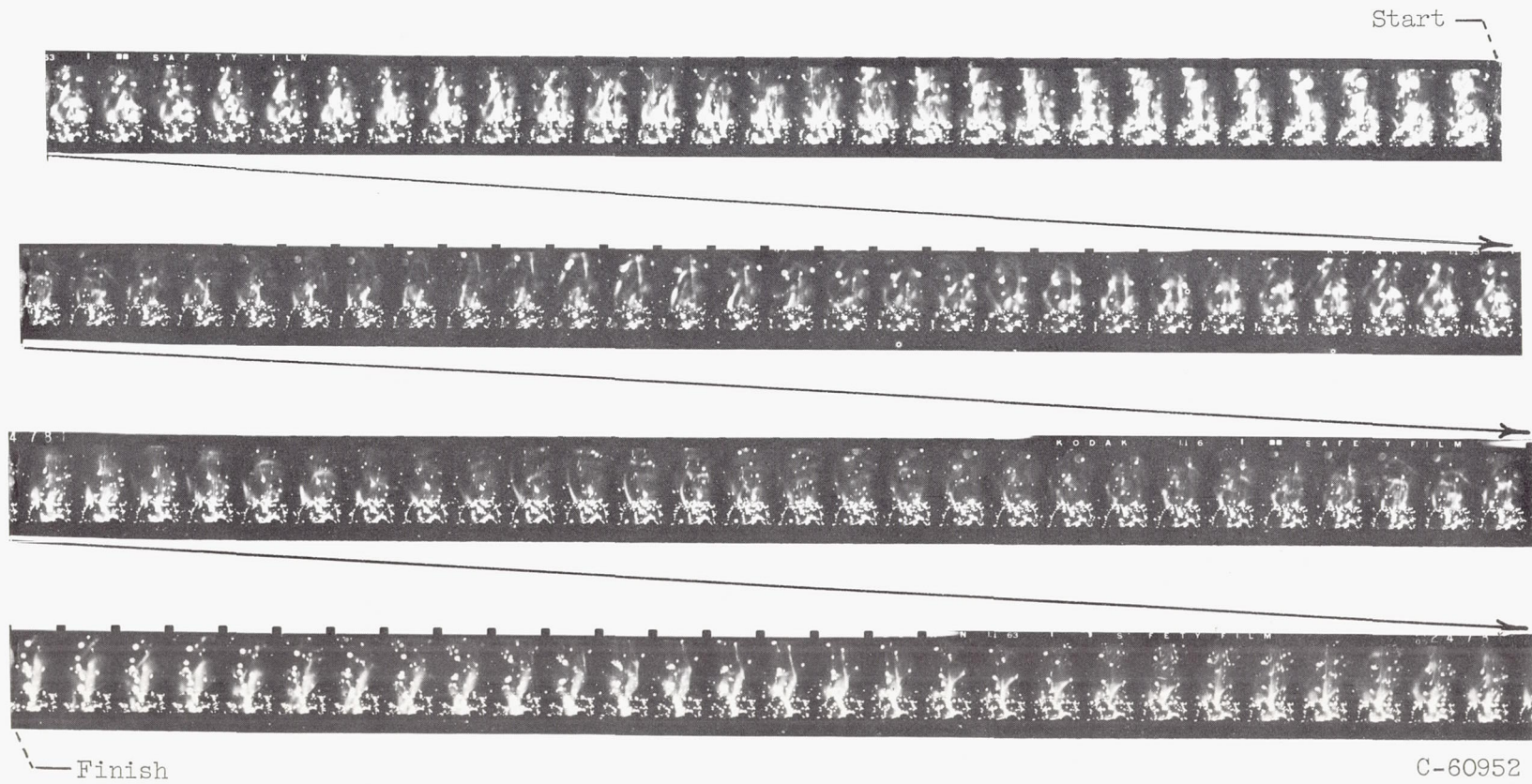
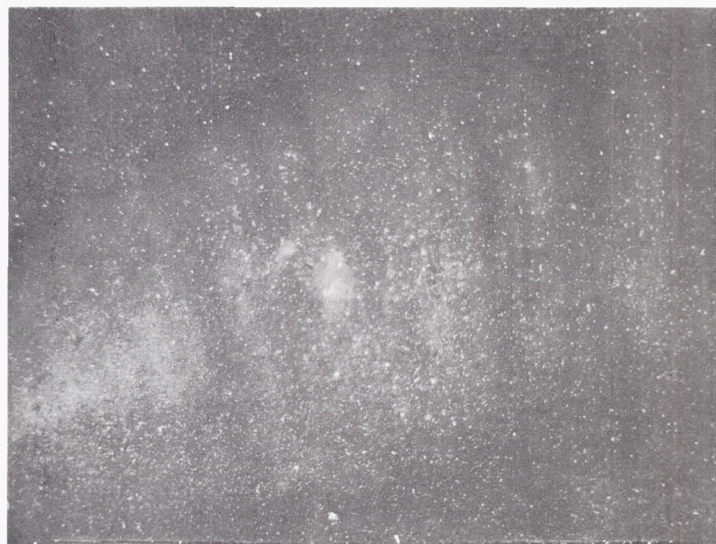


Figure 6. - High-speed photographs of burning surface. Predominantly coarse oxidizer propellant l. f8.0, tri-X film, 3200 frames per second.



(a) Predominantly fine oxidizer propellant.



C-59477

(b) Predominantly coarse oxidizer propellant.

Figure 7. - Photomicrographs of combustion products. X13.

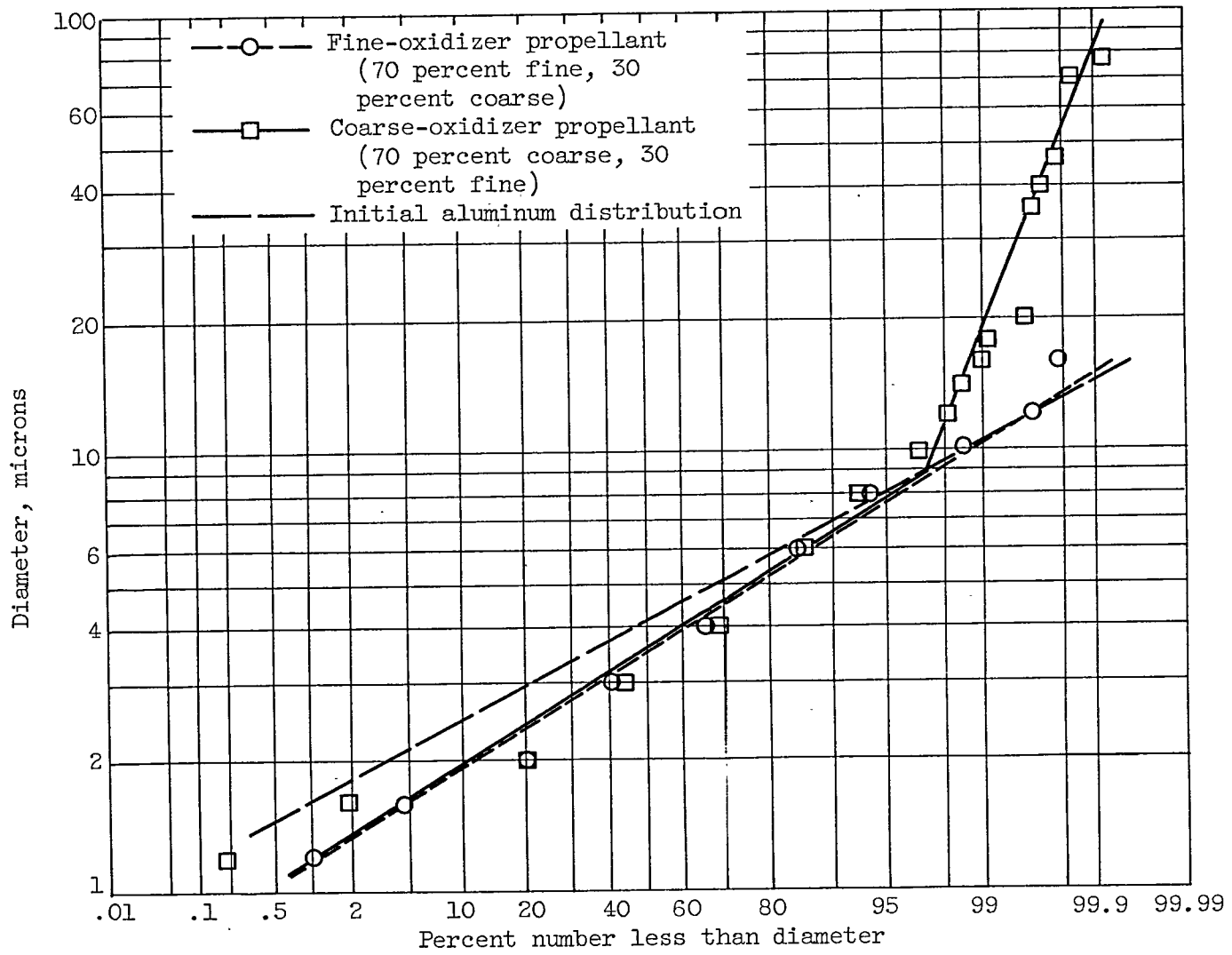
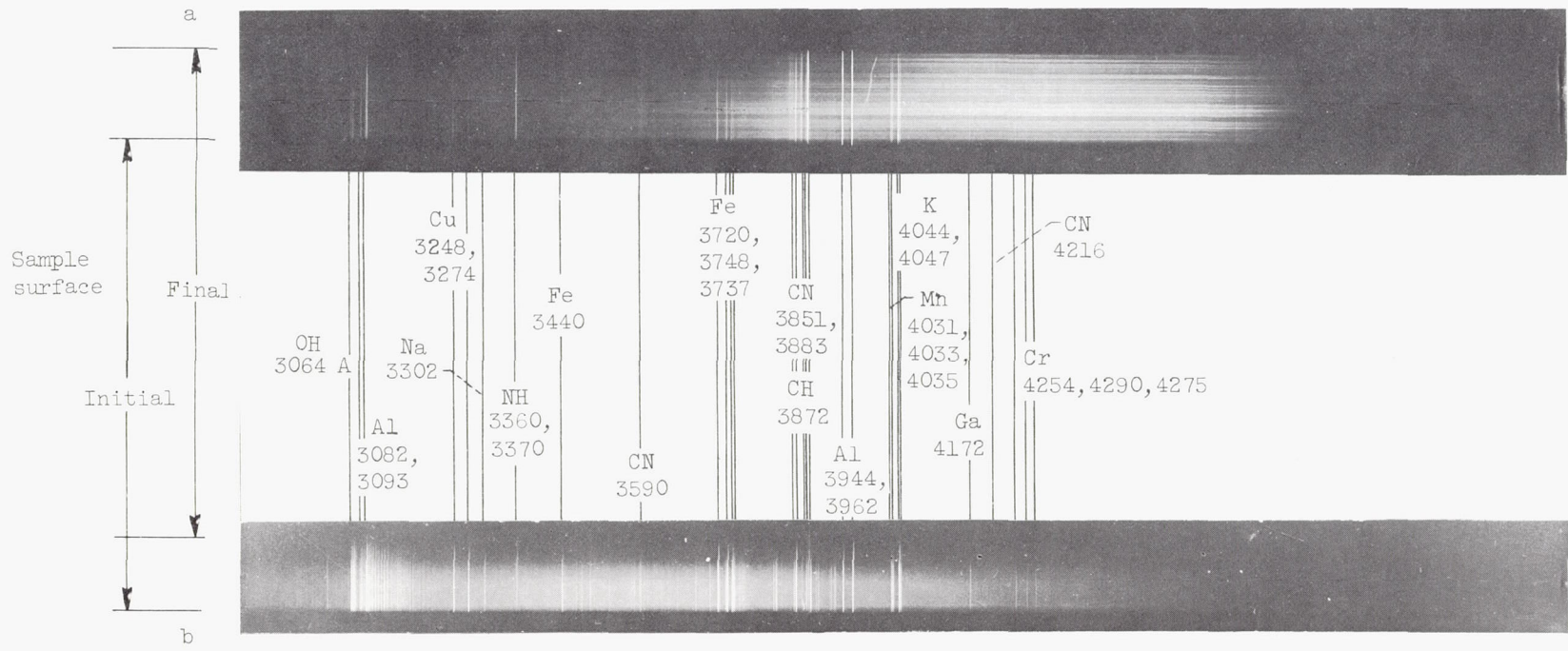


Figure 8. - Combustion-product size distribution.

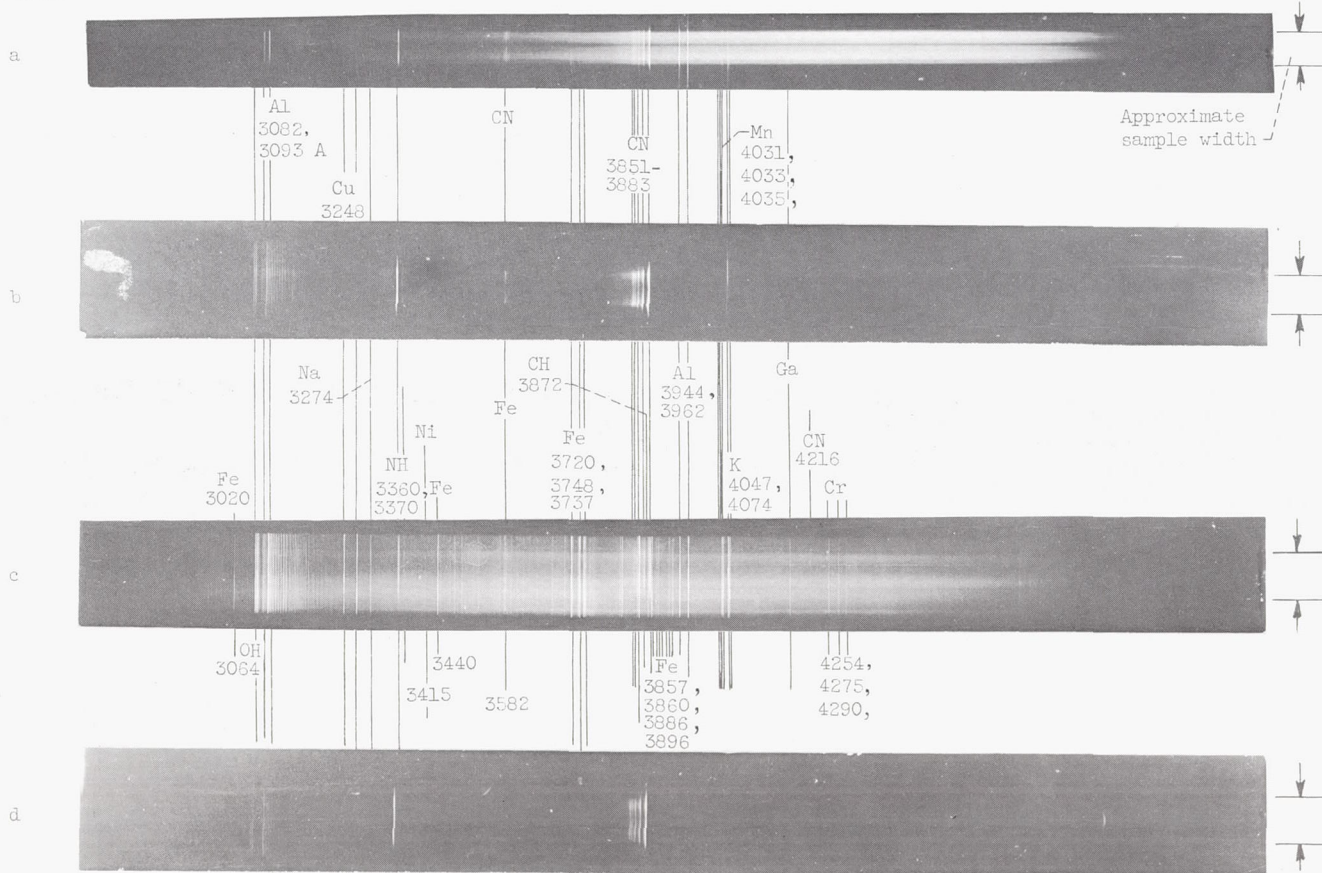


C-60950

- (a) Coarse-oxidizer propellant 1.
- (b) Fine-oxidizer propellant 2.

Figure 9. - Spectra of burning propellant samples with optical arrangement 1 of figure 5(b). Film type, Eastman I-O; exposure, 7 seconds; spectrographic slit, 150 microns. (Spectra rotated 180° from position shown in fig. 5(b), arrangement 1.)

Spectrum



(a) Coarse-oxidizer propellant 1; percent of Al, 9.

C-60951

(b) Coarse-oxidizer propellant 3; percent of Al, 0.

(c) Fine-oxidizer propellant 2; percent of Al, 9.

(d) Fine-oxidizer propellant 4; percent of Al, 0.

Figure 10. - Spectra of burning propellant samples (table I) with optical arrangement 2 of figure 5(b). Film type, Eastman I-O, exposure, 7 seconds; spectrographic slit, 150 microns.